# Imaging of Stress Fractures

5

Jason E. Payne and Joseph S. Yu

## Introduction

Athletes are particularly prone to injuries that are related to overuse. In the general athletic population, the incidence of stress fractures is about 1 % but may vary according to activity, for instance, up to 20 % in runners [1, 2]. The location where a stress fracture develops also is specific to a particular sporting activity [3, 4]. It is reported that 60 % of athletes presenting with a stress fracture have experienced a prior stress fracture [5]. In the osseous tissues, overuse injuries produce stress-induced changes that may alter the architecture of the bone. Stress is defined as any force or absolute load that is applied to a bone. These forces arise from having to bear unusual weight or repetitive load, or are created when there is an imbalance of muscles [6–8]. Wolff's Law dictates that a change in the mechanical environment of a bone from new or intermittent stress elicits the remodeling of the osseous architecture of that bone to adjust to its new environment [9]. Increases in muscular strength often precede strengthening of the bone, and this can create an imbalance between the relative strength of these tissues. Furthermore, when muscles fatigue during exercise, the protective effect of muscle tension diminishes reducing the ability of bone to resist stress.

A stress fracture represents unsuccessful adaptation by a bone under duress [10, 11]. Stress fractures are generally divided into two categories. *Fatigue* stress fractures occur when normal bone is subjected to repetitive stresses that lead to mechanical failure as a consequence of inadequate remodeling of microfractures. An example of this occurs when an athlete abruptly changes a training regimen, not allowing sufficient time for bone to remodel in response to the added stress. *Insufficiency* fractures occur when normal stresses are applied to an abnormal or pathologic bone that is incapable of adaptation. Fatigue stress fractures related to overuse are relatively common in certain groups, particularly athletes and military personnel [12, 13]. The incidence of stress fractures among females in the military tends to be higher than in men, but this difference has not been consistently observed in athletes [14–17]. The most common pathologic bone abnormality in older athletes that increases the risk for stress fractures is osteoporosis, with the highest reported prevalence occurring in postmenopausal women [18, 19]. A variety of other conditions associated with abnormal underlying bone also predispose an athlete to insufficiency

J.E. Payne, MD
Musculoskeletal Division, Department of Radiology, Wexner Medical Center at The Ohio State University, 395 W 12th Ave Ste 460, Columbus, OH 43210, USA
e-mail: Jason.payne@osumc.edu

J.S. Yu, MD (✉)
Department of Radiology, The Ohio State University Wexner Medical Center, 395 West 12th Avenue, Suite 481, Columbus, OH 43210, USA
e-mail: joseph.yu@osumc.edu

T.L. Miller and C.C. Kaeding (eds.), *Stress Fractures in Athletes: Diagnosis and Management*,
DOI 10.1007/978-3-319-09238-6_5, © Springer International Publishing Switzerland 2015

fractures including rheumatoid arthritis, corticosteroid use, and diabetes mellitus [20, 21].

Forces resulting in osseous injury can be classified as compression, tension, and/or shear. It is useful to consider these forces when assessing the morphologic properties of a stress fracture. For instance, distant runners tend to develop stress fractures in the posteromedial aspect of the tibia owing to repetitive compressive forces whereas dancers and jumping athletes tend to develop tibial stress fractures in the anterior tibial shaft due to tensile forces.

## Evolution of Imaging

The imaging appearances of stress-induced injuries change over time and the rate of change is affected by factors such as the bone involved, location of injury, inciting activity, and age [22]. The sensitivity of radiography for early diagnosis of stress fractures is low because forces tend to distribute along long segments of the cortex producing subtle changes at the surface of the bone and the periosteum [13, 18]. This early phase is referred to collectively as a stress response or stress reaction. If the cyclic loading continues, progressive deformation of the bony architecture localizes to a focal weakened area of the bone resulting in a uni-cortical break in the cortex, or a true stress fracture. Athletes who develop fatigue fractures often exhibit the following triad: a new or different activity has been introduced in their training, the activity is strenuous, and the activity is repeated cyclically. In a stress reaction, there is still active healing of the microfractures but in a stress fracture, the progressive forces ultimately exceed the elastic range of the bone leading to structural failure.

Stress fractures account for at least 10 % of patients encountered in a typical sports medicine practice [1]. Imaging has traditionally provided diagnostic support for evaluation of these patients with modalities depicting variable sensitivity and specificity according to the stage along the continuum of a stress injury [23]. Radiography continues to be a low-cost frontline technique but is limited by a lack of sensitivity especially early in the process. The first effective modality to have an impact on the diagnosis of osseous stress injuries was whole body bone scintigraphy utilizing technetium-99m-methylene diphosphonate (Tc-99m-MDP). Stress fractures are visible on bone scans days to weeks earlier than radiographs. For many years, it served as the gold standard for early confirmation of stress-induced changes related to increased bone metabolism and osteoclastic activity. The limitation of bone scintigraphy was that it lacked specificity in areas that ordinarily resulted in an increase in radiopharmaceutical uptake, however, the advent of triple-phase scanning with additional angiographic and blood pool phases contributed to improved specificity [24].

Although computed tomography (CT) has shown superior spatial resolution in comparison to other imaging modalities, its role in evaluating patients with stress fractures continues to be limited. Recently, however, utilization of multidetector CT has increased due to the ability to depict the stress fracture line in coronal and sagittal high-resolution multiplanar-reconstructed CT images as well as 3D volume rendered images [25]. This has increased the utilization of CT for differentiation of stress fractures from other entities such as osteoid osteoma which may have similar radiographic appearances. Ultrasound also has a limited role in the diagnosis of stress-related injuries although it has the ability to assess the superficial cortical surface in bones close to the skin as well as fracture lines, periosteal reactive changes including callus formation, edema in periosseous tissues, and increased perfusion [26, 27].

Most recently, magnetic resonance imaging (MRI) has been shown to be extremely sensitive to the pathophysiologic changes that are associated with stress-induced conditions and provides greater specificity than radionuclide imaging owing to its superior spatial resolution [28, 29]. MRI has been efficacious in characterizing early changes of stress injuries with high sensitivity and specificity to local hyperemia and edema, periostitis, bone marrow changes, and cortical failure and is considered the current gold standard [30]. It also has been useful in estimating clinical severity, guiding therapy, and estimating the duration of disability [31].

## Imaging Techniques

### Radiography

The initial workup of an athlete with pain should begin with a radiographic evaluation of the area involved. Because the initial imaging features of a stress fracture are subtle, radiographs should be done with precision (optimal positioning) and in a comprehensive manner, i.e., with all required projections, and accompanied with a proper history. Accuracy is increased when the radiographs are optimized and a reliable search strategy is employed [32]. A common approach is to critically evaluate the integrity of the cortex for changes in density (Fig. 5.1), as well as for periosteal reactive and endosteal reactive changes (Fig. 5.2). The medullary cavity should be assessed for the presence of impacted trabeculation and linear uni-cortically based sclerotic bands. Other findings include transverse or longitudinal breaks in the cortex (Fig. 5.3) as well as trabecular angulation and distraction which may be a manifestation of progression (Fig. 5.4). Altered cortical morphology which may be either focal thickening or thinning is usually an indication of a chronic condition.

It is important to realize that the location and orientation of developing stress fractures influence the radiographic appearance so that fractures at the ends of tubular bones tend to depict linear areas of sclerosis whereas fractures in the shaft of a tubular bone may be simply a lucent cortical break or focal periostitis [33]. Longitudinal stress fractures have the appearance of a thickened cortex with a vertically oriented lucency in the cortex (Fig. 5.6). In bones composed largely of cancellous bones such as the tarsus and femoral neck, the first sign of a stress fracture may be simply focal linear sclerosis (Fig. 5.7). In these cases, initial findings are subtle blurring of the trabecula secondary to microfractures. As healing of the microfractures progresses, linear sclerosis

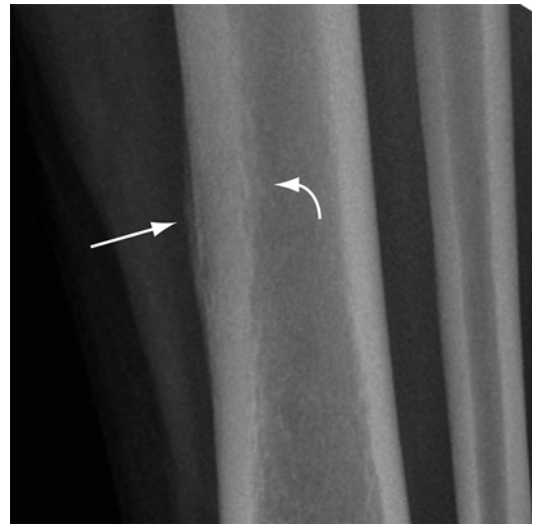

**Fig. 5.2** Chronic radiographic findings of stress response. Close up of radiograph of the mid-tibia shows mature periosteal (*arrow*) and endosteal reactive changes (*curved arrow*) associated with focal areas of osteopenia in the cortex

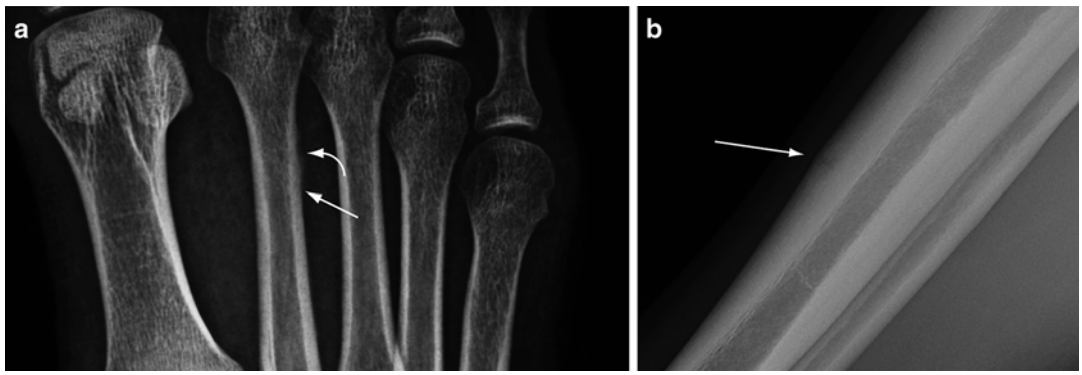


**Fig. 5.1** Early stress response on radiography. (**a**) Frontal radiograph of the forefoot shows focal osteopenia of the lateral cortex of the distal second metatarsal shaft (*white arrow*) and periostitis (*curved arrow*). (**b**) Lateral radiograph of the tibia shows focal cortical osteopenia (*arrow*)

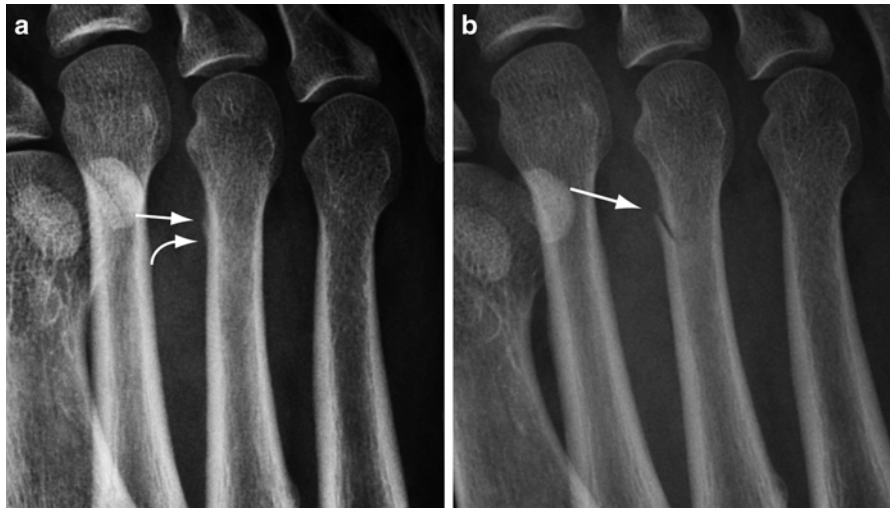


**Fig. 5.3** Radiography of early stress fracture. (**a**) Oblique radiograph of the forefoot shows periostitis of the medial cortex of the third metatarsal shaft (*arrow*) and a subtle lucency (*curved arrow*) representing the start of a break in the cortex. (**b**) Follow-up image in 3 weeks shows completion of the cortical fracture with oblique lucency (*arrow*)


**Fig. 5.4** Stress fracture progression. (**a**) Oblique forefoot radiograph in one patient shows a classic Jones stress fracture involving the lateral cortex of the proximal fifth metatarsal shaft (*arrow*). The fracture was isolated to the cortex. (**b**) Another patient with a Jones stress fracture shows extension into the medullary cavity after the athlete felt a "pop" while running

appears oriented perpendicular to the course of the trabecular with extension to one cortical surface. Radiographic detectable changes usually become conspicuous weeks to months after the onset of symptoms and the timing and nature of the changes varies with the level of activity. However, it is noteworthy that imaging findings may not be necessarily sequential.

The sensitivity of radiographs for early stress fractures is as low as 15 % and follow-up radiographs may demonstrate findings in only 50–54 % of cases [7, 34]. Development of subsequent radiographic findings is often determined by whether there is cessation of the inciting stress that is affecting the bone. Prior studies comparing radiography to bone scintigraphy have reported a

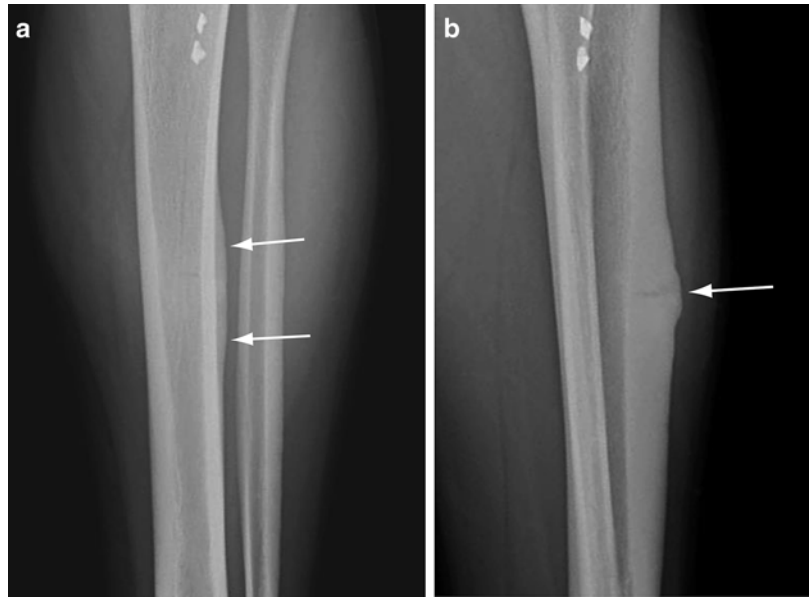


**Fig. 5.5** Striated stress fracture. (**a**) Frontal radiograph of the tibia shows periosteal elevation along the anterolateral cortex of the mid-tibia (*arrows*). (**b**) Lateral view shows a transverse lucency through the cortex with more pronounced periosteal reaction directly adjacent to the fracture (*arrow*)

**Fig. 5.6** Radiography of longitudinal stress fracture. Frontal radiograph of the femur shows a linear lucency (*arrows*) within the medial femoral cortex oriented along the longitudinal axis of the bone

sensitivity of 56 %, a specificity of 94 %, an accuracy of 67 %, positive predictive value of 95 %, and a negative predictive value of 48 % [28]. There are many classifications available for grading the radiographic features of stress fractures but currently none have been ubiquitously utilized [35, 36].

Tomosynthesis, or digital radiography, has recently been shown to be superior to conventional radiography in detection of occult fractures and it may have an application in the evaluation of stress fractures [37]. This new imaging technique can depict both cortical as well as trabecular changes, so its performance is considered only slightly lower to that of CT but at lower radiation exposure [38].

The differential diagnosis for stress fracture on radiography is limited particularly as specificity of the study increases in the chronic phase of the fracture. Chronic osteomyelitis may present with periosteal and endosteal reactive changes resulting in cortical thickening but clinically, these two entities are not at all similar. Occasionally, a stress fracture may mimic a tumor [39]. Osteoid osteoma may result in cortical thickening and reactive bone formation and is often encountered in a similar patient population as stress fracture. The presence of a central lucent nidus as well as a less linear pattern of sclerosis and clinical history can aid in differentiation.

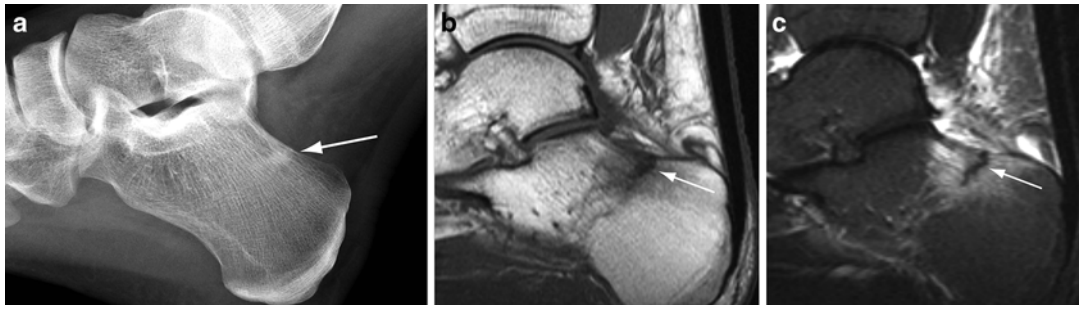


**Fig. 5.7** Stress fracture in cancellous bone. (**a**) Lateral radiograph of the calcaneus demonstrates a linear area of sclerosis perpendicular to the trabeculation in the superior calcaneus (*arrow*). Sagittal T1-weighted (**b**) and STIR (**c**) MR images show a uni-cortical, low-signal fracture line (*arrows*) surrounded by intense bone marrow edema

## Radionuclide Scintigraphy

Bone scintigraphy had for many years been regarded as the gold standard for evaluating stress-induced injuries and although recently supplanted by MRI, it continues to be widely utilized in many situations. It measures bone response to injury by depicting areas of increased osseous metabolism through the localization of radionuclide tracers, particularly Tc-99m-MDP. The degree of uptake depends on the rate of bone turnover and local blood flow, and abnormal uptake may be seen within 6–72 h of injury [7, 34, 40]. Whole body bone scans can be performed with relatively low cost and have the advantage of being able to image the entire skeletal system at once, which is useful in cases when more than one area is symptomatic. The sensitivity of bone scintigraphy is nearly 100 % [7].

The specificity of bone scintigraphy, however, is limited by any process that increases blood flow and has osteogenic activity such as arthritis, infection, malignancy, infarctions, and metabolic conditions. The specificity can be improved by performing a three-phase study [24]. The first phase includes a dynamic flow study with images obtained at 1 s intervals for 60 s after the injection of radiopharmaceutical and is followed by a static "blood pool" image (second phase) obtained a few minutes later. These phases depict vascularity and soft tissue involvement, respectively. The third phase is the standard 2- to 4-h delayed images depicting the osteoblastic response. An acute stress fracture will be positive in all three phases while a chronic stress fracture tends to show activity only on the delayed images [7]. Another limitation of scintigraphy in patients with stress fractures is that the scintigraphic abnormality may take 4–6 months to resolve rendering the modality inadequate for sequential follow-up studies [41]. Several grading schemes are available to characterize the severity of a stress fracture according to its scintigraphic features.

The characteristic scintigraphic appearance of a stress fracture in delayed static images is intense, fusiform cortical uptake along the long axis of the bone at the level of the fracture (Fig. 5.8) [42]. However, there can be a wide spectrum of findings representative of the pathophysiologic continuum of the process and the variations in the orientation of the fracture such as in a longitudinal fracture (Fig. 5.9). A stress reaction is manifested by an area of less intense radionuclide uptake along the cortex corresponding to areas of remodeling bone during the period that radiographs are typically normal.

Athletes who are involved in rigorous training regimens may present with multiple symptomatic regions of bone that show abnormal radionuclide uptake, and these findings have been shown to represent both stress reaction and frank stress fractures. However, some patients also depict abnormal uptake in regions of bone that are not symptomatic. This likely represents the earliest manifestation of bone remodeling

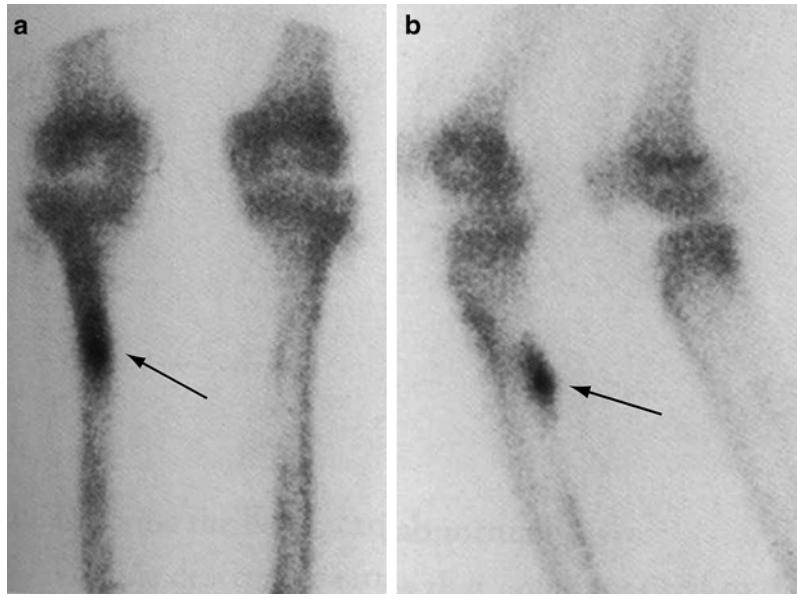


**Fig. 5.8** Typical scintigraphic findings of a stress fracture. Delayed static images of the tibia from a whole body bone scan utilizing Tc-99m-MDP in the frontal (**a**) and oblique (**b**) projections show a characteristic appearance of a stress fracture in the tibia depicted as a fusiform region of radionuclide uptake oriented along the long axis of the bone (*arrows*)

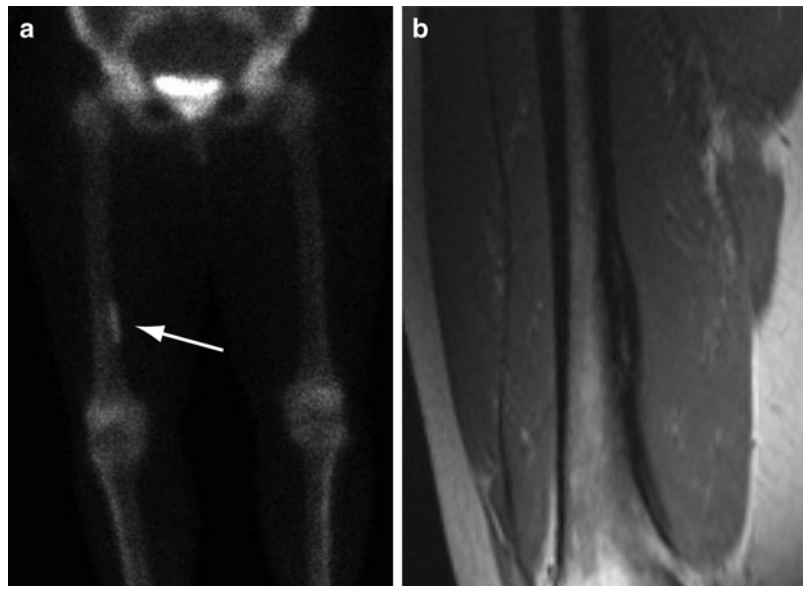


**Fig. 5.9** Longitudinal stress fracture on scintigraphy. (**a**) Delayed frontal static bone scan image utilizing Tc-99m-MDP shows a thin, linear area of increased activity in the medial cortex of the distal right femoral shaft (*arrow*). (**b**) Coronal T1-weighted MR image shows a longitudinal stress fracture depicted as a linear area of intermediate signal intensity within the thickened cortex aligned to the axis of the bone

[43]. The asymptomatic foci have been reported in as high as 46 % of subjects in one series [44]. With continued activity, these may progress to symptomatic stress injuries.

The application of planar scintigraphy in combination with single-photon emission computed tomography (SPECT) has been recently advocated for increasing the accuracy of grading stress fractures. In a recent study evaluating patients with known femoral neck stress fractures diagnosed with MR imaging, the sensitivity of planar scintigraphy alone was reported to be 50 % while the sensitivity for planar scintigraphy in combination with SPECT increased to 92 % [45]. Similarly, the accuracy for scintigraphy alone was 12.5 % but increased to 70 % when SPECT was added. SPECT has also been shown to improve the diagnostic accuracy of stress fractures at the pars interarticularis region of the spine, a process that is commonly observed in adolescent athletes with back pain. SPECT has been shown to provide more detailed anatomic depiction of the region in comparison to MRI and higher sensitivity in comparison to planar scintigraphy alone [46–48]. However, SPECT is limited in the spine owing to a high rate of false positives and false negatives [49].

## Ultrasound

Sonography has a very limited role in the evaluation of stress fractures and is not recommended as a stand-alone study [50]. However, studies have shown that this modality may occasionally be used to assess the superficial surface of the cortex in bones that are located close to the skin such as in the ankle/feet and tibia [51]. Cortical irregularities such as periostitis and callus formation can be depicted as well as muscular edema around the bone, and compression of the probe is useful in confirming pain. Color Doppler imaging can demonstrate areas of hyperperfusion at and near the stress fracture.

Recent studies have demonstrated a sensitivity of 82 % and a specificity of 67–76 %, but predictive values offer a wide range with studies reporting a 59–99 % positive predictive value and a 14–92 % negative predictive value [26, 52].

## Computed Tomography

The role of CT in the assessment of stress-related injuries continues to be relatively limited despite advances in technology. CT is less sensitive than both MRI and nuclear scintigraphy in depicting the early changes of bone remodeling from repetitive stress [7, 29, 31]. However, the ability to produce thin-section, multiplanar-reconstructed images in order to provide high resolution and detailed depiction of cortical bone does relegate CT to an important adjunctive role when the imaging features in other modalities are equivocal [53]. CT is clearly superior to both sonography and conventional radiography. The earliest finding of a stress injury on CT is focal cortical osteopenia, but this is not a common observation because CT is typically not a first-line study (Fig. 5.10). CT manifestations that are distinctive of stress injuries, however, include thickening of the cortex, periosteal reactive changes, intramedullary sclerosis, and longitudinal and transverse lucent fracture lines. The main limitation of CT is that these findings may not develop until the patient has been symptomatic for several weeks. However, high-resolution CT is currently the most sensitive modality for detecting subtle cystic

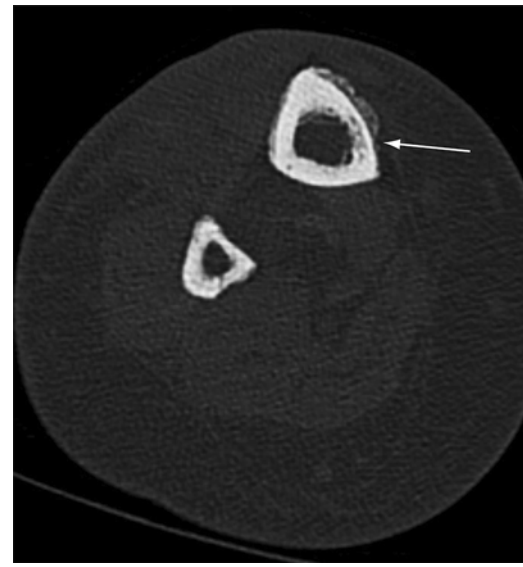

**Fig. 5.10** Computed tomography, early stress response. Axial CT image of the tibia shows focal osteopenia in the cortex of the bone (*arrow*) where it is undergoing stress-induced changes

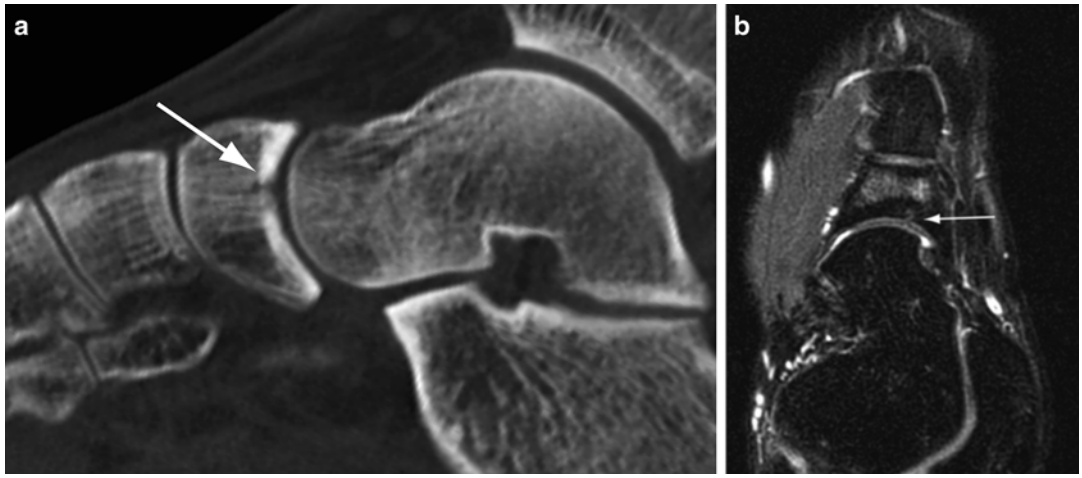


**Fig. 5.11** Cortical resorption cavity. (**a**) Sagittal multiplanar CT image of the foot shows focal osteopenia in the cortex at the point of the fracture (*arrow*) indicating a developing cortical resorption cavity. (**b**) Axial STIR MR image shows the cystic defect in the cortex (*arrow*) and bone marrow edema in the medullary space

changes in the cortex that characterize cortical resorption cavities (Fig. 5.11). Once a fracture line in the cortex develops, the defect is easily demonstrated by conventional axial images as well as by multiplanar reformatted or 3D volume rendered images (Fig. 5.12) [54].

CT is advantageous in certain situations over other imaging techniques. It is useful in differentiating healing from progression (Figs. 5.13 and 5.14). Certain location-specific conditions are better suited for CT. Stress fractures that affect the tarsal navicular are often difficult to diagnose because the symptoms associated with this condition are often vague and there may be a paucity of specific physical findings [55]. Additionally, the overall density of the navicular can, in part, obscure the linear focus of sclerosis that accompanies a stress fracture on radiography. In these cases, CT is useful in elucidating the imaging characteristics of the stress fracture such as the extent of abnormality, orientation, and if there are indicators of avascular necrosis. A similar challenge may occur in patients with pars interarticularis fractures. Fracture lines are often difficult to visualize utilizing other modalities such as MRI but are clearly illustrated on CT [49, 56]. Occasionally, cortical thickening may be a nonspecific finding. For instance, the radiographic manifestation of an osteoid osteoma may mimic those of a stress fracture because both conditions thicken the cortex and are associated with variable periosteal reactive changes. By utilizing thin-section CT images, these entities can be reliably differentiated by the identification of the lucent nidus that is the classic feature of osteoid osteoma within the region of cortical thickening and sclerosis [57]. The power of CT over MRI is in its ability to penetrate the high-attenuation cortical bone. Although MRI remains the single best method for evaluating early stress injuries, it is relatively insensitive to changes that occur only within the cortex. Therefore, the subset of cortical stress injuries that are characterized by osteopenia, resorption cavities, and striations are better suited for evaluation by CT [58]. Longitudinal stress fractures of the tibia caused by repetitive torsional loading in runners are another subset of fractures that are best evaluated with CT. The longitudinal orientation and extension of the fracture negates the effectiveness of radiographs and though MRI is capable of depicting the abnormality, CT has been reported to be more sensitive in identifying the fracture line itself [59].

Peripheral quantitative computed tomography (pQCT) is a CT technique that has demonstrated potential in the evaluation of stress fractures by the acquisition of high-resolution images of the extremities at lower radiation doses than with conventional CT. The pQCT

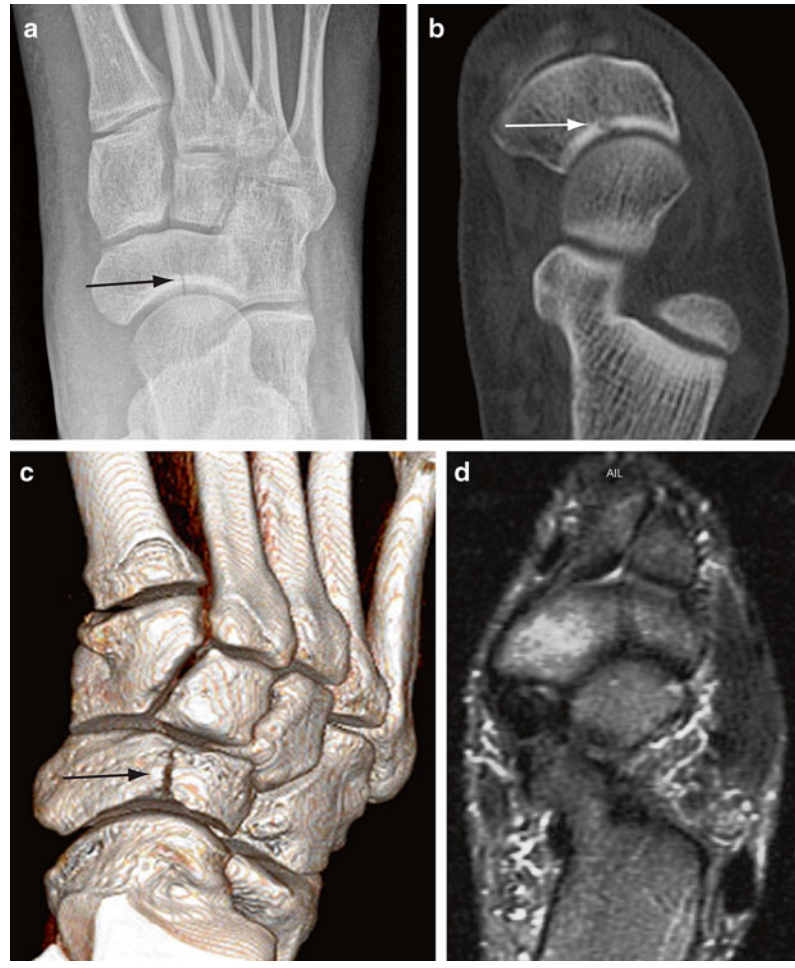


**Fig. 5.12** Subacute navicular stress fracture. (**a**) Frontal foot radiograph of a college basketball player shows a vertical lucency (*arrow*) in the lateral aspect of the navicular. (**b**) Axial multiplanar CT image confirms the stress fracture (*arrow*) as well as normal bone density throughout the tarsal bone. (**c**) 3D volume rendered CT image depicts the entire stress fracture (*arrow*) in one image. (**d**) T2-weighted MR image demonstrates bone marrow edema in the medial and lateral bone fragments

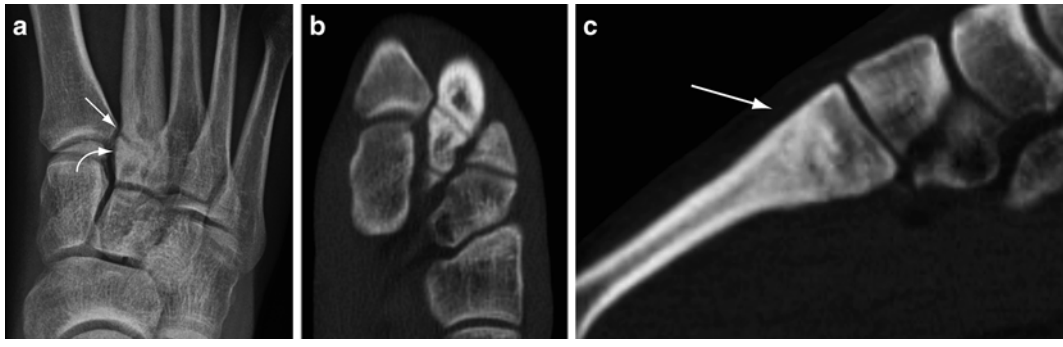


**Fig. 5.13** Chronic stress fracture. (**a**) Frontal radiograph of the foot demonstrates a transverse lucency near the base of the second metatarsal bone (*arrow*). Sclerosis adjacent to the fracture is evident (*curved arrow*). Axial (**b**) and sagittal (**c**) multiplanar CT images more optimally characterize the stress fracture and also shows that the dorsal cortex is intact (*arrow*)

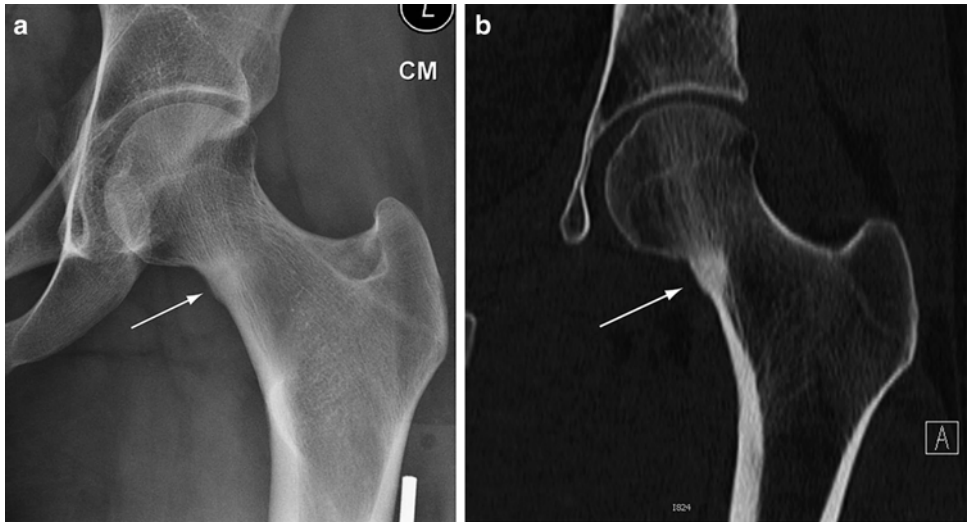


**Fig. 5.14** Computed tomography of healing stress fracture. (**a**) Frontal radiograph of the hip shows a region of sclerosis on the compressive side of the femoral neck with focal periosteal reactive changes (*arrow*). (**b**) Coronal multiplanar CT image shows that the fracture line has nearly filled in and is no longer evident (*arrow*)

images afford detailed portrayal of the structure and mineralization of bone at the location of the stress fracture. As such, it may have application in monitoring the stress fracture throughout the healing phase [60, 61].

## Magnetic Resonance Imaging

MRI is currently the gold standard for diagnosing and classifying stress-induced injuries. Several important features of this imaging modality have contributed to its emergence as a superior tool for assessing these conditions including unparalleled contrast, outstanding spatial resolution particularly with higher strength magnets, and the capability to image in an infinite number of geometric planes [62]. Additionally, it does not utilize ionizing radiation which is ideal in the athletic population who tend to be younger [63]. MR images, in general, can be obtained in a shorter period of time than with a scintigraphic examination, and provides images that are exquisitively sensitivity to the subtle changes seen in patients with early stress fractures. Numerous studies have shown that MRI outperforms radiography, CT, and radionuclide scanning [28, 29, 31, 64, 65].

MRI examinations are optimized by utilizing dedicated coils which serve to increase the signal-to-noise ratio and decrease artifacts. Higher strength magnets, such as 3-T systems which are becoming more commonplace, offer higher spatial and contrast resolution, shorter scanning times, and improved conspicuity of bone marrow edema than conventional 1.5-T systems [66]. The sensitivity is comparable for both MR systems and routinely, 1.5 T MR images are typically adequate for diagnosis and characterization of stress fractures [67, 68]. Typical sequences applied include short tau inversion recovery (STIR), which is commonly used in screening since it has the highest sensitivity to edema, and fast spin-echo sequences with fat-saturation which are excellent in preserving high spatial resolution. A T1-weighted sequence is generally prescribed to further characterize the inherent signal intensity of lipoid marrow. Intravenous gadolinium is not frequently administered in the evaluation of stress fracture. However, dynamic enhancement has been reported in patients with higher grade stress reactions and stress fractures caused by increased tissue perfusion. This may be useful in cases where the pre-contrast MR images show a callus, fracture, or muscle edema,

and in situations where there is a concomitant malignancy or infection [69].

MRI is an effective diagnostic technique in patients who show strong clinical manifestations of a stress fracture but have normal initial radiographs [70, 71]. Like scintigraphy, MRI depicts changes in the bone and periosteum weeks before any radiographic abnormality develops. The early stages of a stress fracture are characterized by focal hyperemia and bone marrow edema that correlates with the development of microfractures and osseous resorption. Endosteal reactive changes, periostitis, and periosseous edema are important early observations on STIR or T2-weighted spin-echo images, and are characteristic of stress reactions (Fig. 5.15) [65, 72]. Edema appears bright in signal intensity on these sequences. Focal periosteal elevation develops as the process becomes more severe (Fig. 5.16). As the injury progresses and becomes more severe, marrow edema appears on T1-weighted images as areas of low-signal intensity (Fig. 5.17). As breakdown of the cortical bone progresses, a frank stress fracture forms either transversely or longitudinally (Figs. 5.18 and 5.19) [64]. The most common patterns of a fatigue stress fracture on MRI are a linear, uni-cortically-based abnormality of low-signal intensity surrounded by a larger, ill-defined region of marrow edema, or a linear cortical abnormality with adjacent muscular or soft tissue edema [73–75]. Callus formation indicates a more chronic stress fracture. The MRI features in the continuum of a developing stress fracture parallel to those that are observed on bone scintigraphy.

Reportedly, MRI has comparable sensitivity to nuclear scintigraphy. Specificity, accuracy, positive predictive value, and negative predictive value are all superior at 100 %, 90 %, 100 %, and 62 %, respectively [29]. Additionally, MRI has a distinct advantage by depicting the surrounding soft tissue structures thus permitting concomitant evaluation of muscular, tendinous, or ligamentous structures. In the athletic population,

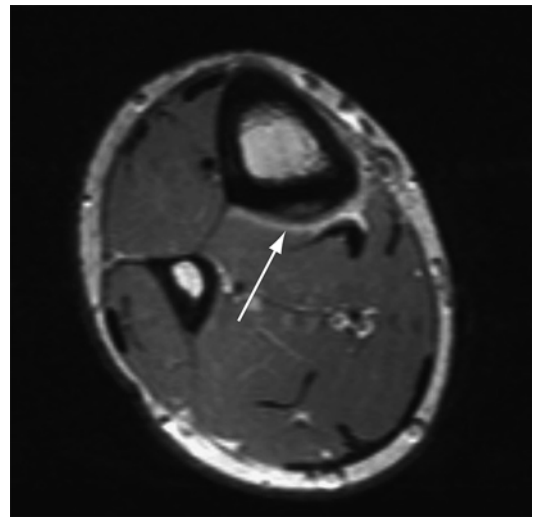

**Fig. 5.16** MR of chronic stress reaction. Axial proton-density MR image shows periosteal elevation in the posterior cortex of the tibia (*arrow*) and adjacent inflammation

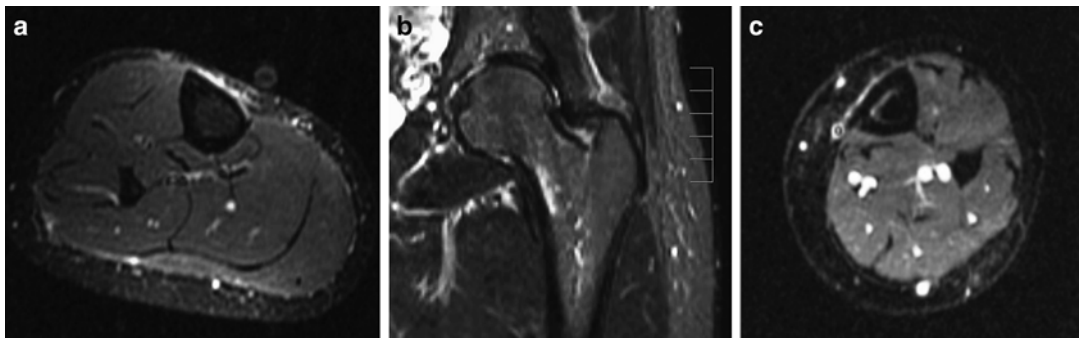


**Fig. 5.15** Different stress responses on MR imaging. Fluid-sensitive MR images in three different athletes. (**a**) Periostitis along the medial cortex of the tibia manifests as linear high-signal intensity along the outer cortex. (**b**) Endosteal reaction with marrow edema along the endosteal surface of the femoral neck. (**c**) A patient with a more severe stress response shows both periosteal and endosteal reactive changes

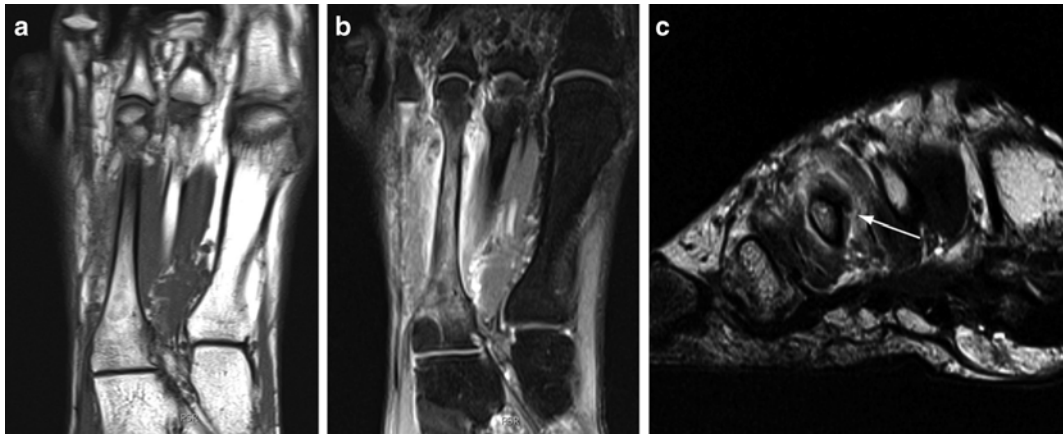


**Fig. 5.17** MR features of developing stress fracture. (**a**) Axial T1-weighted MR image shows low-signal intensity bone marrow in the third metatarsal bone from edema. (**b**) Corresponding T2-weighted image shows adjacent periosteal inflammation shown as linear high-signal intensity fluid along the cortex on both sides of the bone. (**c**) There is rupture of the medial periosteum (*arrow*) and edema in the surrounding interosseous muscle

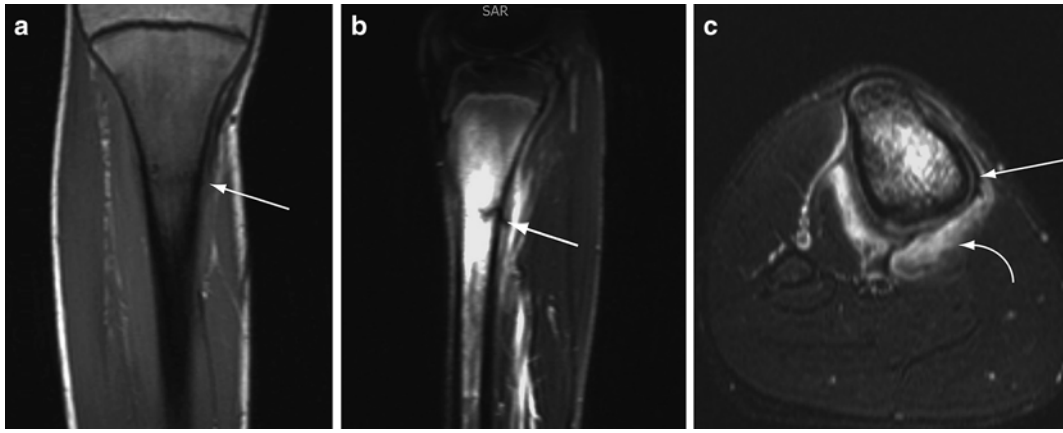


**Fig. 5.18** Typical stress fracture on MR imaging. Coronal T1-weighted (**a**) and sagittal STIR (**b**) images of the tibia show marrow edema and periostitis as well as edema in the adjacent posterior soft tissues. The transverse stress fracture is low in signal on both sequences (*arrows*) and surrounded by a larger region of marrow edema. (**c**) Axial fluid-sensitive image demonstrates extensive periosteal elevation (*white arrow*) and periosseous soft tissue edema (*curved arrow*)

injuries to any of these structures may mimic the symptoms of a stress fracture, which are sources that reduce the specificity of nuclear scintigraphic studies. Another feature of MRI that should be underscored is its ability to assess regions of the skeleton that are challenging with other imaging modalities. For instance, insufficiency fractures of the pelvis, proximal femur, and superior acetabulum in elderly patients are often difficult to visualize on CT studies but unequivocally demonstrated on MR images (Fig. 5.20) [76, 77]. Femoral neck stress fractures that are optimally shown on MRI may be occult by radiography or scintigraphy. Any delay in diagnosis of these stress fractures increases the potential for completion of the fracture. Lastly, the anatomic detail of stress fractures afforded by MRI allows distinction between different types of stress fractures, such as compressive and tensile type stress fractures of the femoral neck, the latter requiring operative fixation [70, 78].

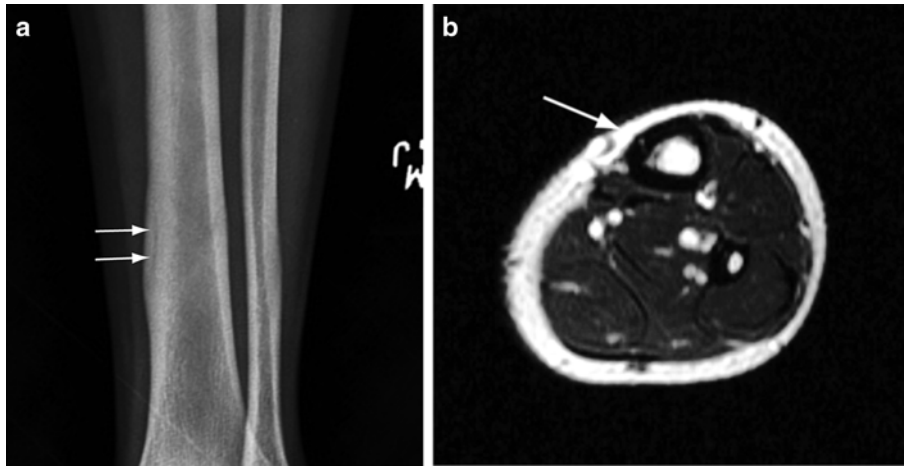


**Fig. 5.19** Longitudinal stress fracture. (**a**) Frontal radiograph of the tibia shows a linear lucency within the thickened medial cortex (*arrows*) in the distal shaft. (**b**) Axial T2-weighted MR imaging shows the vertically oriented break in the cortex (*arrow*)

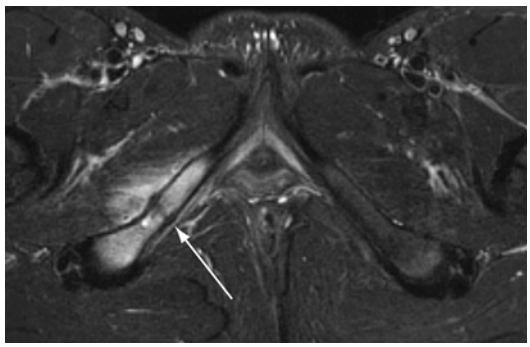

**Fig. 5.20** Pubic ramus stress fracture. Axial STIR image demonstrates a stress fracture of the right inferior pubic ramus (*arrow*) with intense surrounding marrow edema and periosseous edema. The abnormality was radiographically occult due to the oblique orientation of the pubic bone

The majority of proposed grading systems have been for stress injuries of the tibia [41, 79]. Many of the classifications attempt to correlate clinical and imaging findings to those on nuclear scintigraphy but an exact correlation has not been reported to date. Owing to superior spatial and contrast resolution, grading systems that are based on MR findings have shown superior accuracy over other classifications, thus improving the prescription of appropriate clinical management. Also because the clinical impact of varying MR or scintigraphic grades often has no influence on an athlete's ability to return to active participation, some investigators have suggested simplifying the grading systems to reflect findings that have a strong clinical correlation such as the presence of a cortical fracture [29, 58, 80]. For instance, unless a fracture line is present, patients with MR grades ranging from grade 2 to 4a who show variable severity of periostitis and bone marrow edema may be theoretically combined into one grade since the time that the athlete is not permitted to play is similar among these grades, while the development of a fracture, a grade 4b abnormality, requires a prolonged period away from athletic participation and constitutes a more severe grade [80].

The appearances of stress fractures on MRI can occasionally overlap with those of benign and malignant processes [75]. The linear orientation of a stress fracture when it is present helps to differentiate it from the more fusiform cortical thickening that may be observed in a patient with a neoplastic process, or the serpiginous intramedullary appearance that is characteristic of osseous infarctions. In-phase and out-of-phase images utilize the differences in the interaction of water and lipid protons in the magnetic field to assess for the presence of fat and water in areas of bone marrow. Stress fractures and other nonneoplastic processes preserve the fat content of normal

marrow whereas neoplastic processes tend to result in replacement of the fat [81]. Other advanced imaging techniques such as chemical shift imaging, diffusion-weighted imaging, and MR spectroscopy are also available for further tissue characterization when it is required.

The primary limitation of MRI is the cost as it is one of the most expensive imaging techniques available. Utilization must be performed precisely and accurately. False-negative examinations may occur in the setting of technical error such as heterogeneous fat-saturation and partial volume effects, interpretive error, or protocol error by inappropriately selecting the wrong MR sequences. The sensitivity of MRI to edema may result in an errant positive finding if a patient is asymptomatic, so it is important to interpret an examination with proper history and with available correlation to pertinent physical findings [82–84].

## Summary

Radiography remains the initial imaging examination in a patient suspected of having a stress fracture. A number of options are available for further evaluation depending on the phase of the injury but most experts agree that MRI is now the gold standard owing to its superior spatial and contrast resolution, high sensitivity, and specificity to both early and late findings, and the lack of ionizing radiation. When available, MRI should be the next modality employed.

## References


1. Jones BH, Harris JM, Vinh TN, Rubin C. Exercise-induced stress fractures and stress reactions of bone: epidemiology, etiology, and classification. Exerc Sport Sci Rev. 1989;17:379–422.
2. Boden BP, Osbahr DC. High-risk stress fractures: evaluation and treatment. J Am Acad Orthop Surg. 2000;8:344–53.
3. Shindle MK, Endo Y, Warren RF, Lane JM, Helfet DL, Schwartz EN, et al. Stress fractures about the tibia, foot, and ankle. J Am Acad Orthop Surg. 2012;20:167–76.
4. Brukner P, Bradshaw C, Khan KM, White S, Crossley K. Stress fractures: a review of 180 cases. Clin J Sport Med. 1996;6:85–9.
5. Korpelainen R, Orava S, Karpakka J, Siira P, Hulkko A. Risk fractures for recurrent stress fractures in athletes. Am J Sports Med. 2001;29:304–10.
6. Yu SM, Dardani M, Yu JS. MRI of isolated cuboid stress fractures in adults. AJR Am J Roentgenol. 2013;201:1325–30.
7. Anderson MW, Greenspan A. Stress fractures. Radiology. 1996;199:1–12.
8. Belkin SC. Stress fractures in athletes. Orthop Clin North Am. 1980;11:735–42.
9. Chamay A, Tschants P. Mechanical influence in bone remodeling: experimental research on Wolff's law. J Biomech. 1972;5:173–80.
10. Burr DB, Martin RB, Schaffler MB, Raddin EL. Bone remodeling in response to in vivo fatigue microdamage. J Biomech. 1985;18:189–200.
11. Long NM, Zoga AC, Kier R, Kavanagh EC. Insufficiency and nondisplaced fractures of the talar head: MRI appearances. AJR Am J Roentgenol. 2012;199:W613–7.
12. Albisetti W, Peruglia D, De Bartolomeo O, Tagliabue L, Camerucci E, Calori GM. Stress fractures of the base of the metatarsal bones in young trainee ballet dancers. Int Orthop. 2010;34:51–5.
13. Fredericson M, Jennings F, Beaulieu C, Matheson GO. Stress fractures in athletes. Top Magn Reson Imaging. 2006;17:309–25.
14. Brukner P, Bennell K. Stress fractures in female athletes. Diagnosis, management and rehabilitation. Sports Med. 1997;24:419–29.
15. Iwamoto J, Sato Y, Takeda T, Matsumoto H. Analysis of stress fractures in athletes based on our clinical experience. World J Orthop. 2011;18:7–12.
16. Iwamoto J, Takeda T. Stress fractures in athletes: review of 196 cases. J Orthop Sci. 2003;8:273–8.
17. Rauh MJ, Macera CA, Trone DW, Shaffer RA, Brodine SK. Epidemiology of stress fracture and lower-extremity overuse injury in female recruits. Med Sci Sports Exerc. 2006;38:1571–7.
18. Krestan C, Hojreh A. Imaging of insufficiency fractures. Eur J Radiol. 2009;71:398–405.
19. Krestan CR, Nemec U, Nemec S. Imaging of insufficiency fractures. Semin Musculoskelet Radiol. 2011; 15:198–207.
20. Satku K, Kumar VP, Chacha PB. Stress fracture around the knee in elderly patients: a case of acute pain in the knee. J Bone Joint Surg Am. 1990;72: 918–22.
21. Manco LG, Schneider R, Pavlov H. Insufficiency fractures of the tibial plateau. AJR Am J Roentgenol. 1983;140:1211–5.
22. Prescott JW, Yu JS. The aging athlete: part 1, "boomeritis" of the lower extremity. AJR Am J Roentgenol. 2012;199:W294–306.
23. Patel DS, Roth M, Kapil N. Stress fractures: diagnosis, treatment, and prevention. Am Fam Physician. 2011;83:39–46.
24. Sterling JC, Edelstein DW, Calvo RD, Webb II R. Stress fractures in the athlete: diagnosis and management. Sports Med. 1992;14:336–46.

25. El-khoury GY, Bennett DL, Ondr GJ. Multidetector-row computed tomography. J Am Acad Orthop Surg. 2004;12:1–5.
26. Banal F, Gandjbakhch F, Foltz V, Goldcher A, Etchepare F, Rozenberg S, et al. Sensitivity and specificity of ultrasonography in early diagnosis of metatarsal bone stress fractures: a pilot study of 37 patients. J Rheumatol. 2009;36:1715–9.
27. Arni D, Lambert B, Delmi M, Bianchi S. Insufficiency fracture of the calcaneum: sonographic findings. J Clin Ultrasound. 2009;37:424–7.
28. Kiuru MJ, Pihlajamaki HK, Hietanen HJ, Ahovuo JA. MR imaging, bone scintigraphy, and radiography in bone stress injuries of the pelvis and lower extremity. Acta Radiol. 2002;43:207–12.
29. Gaeta M, Minutoli F, Scribano E, Ascenti G, Vicni S, Bruschetta D, et al. CT and MR imaging findings in athletes with early tibial stress injuries: comparison with bone scintigraphy findings and emphasis on cortical abnormalities. Radiology. 2005;235:553–61.
30. Kiuru MJ, Niva M, Reponen A, Pihlajamaki HK. Bone stress injuries in asymptomatic elite recruits: a clinical and magnetic resonance imaging study. Am J Sports Med. 2005;33:272–6.
31. Beck BR, Bergman AG, Miner M, Arendt EA, Klevansky AB, Matheson GO, et al. Tibial stress injury: relationship of radiographic, nuclear medicine bone scanning, MR imaging, and CT severity grades to clinical severity and time to healing. Radiology. 2012;263:811–8.
32. Ashman C, Yu JS, Wolfman D. Satisfaction of search in osteoradiology. AJR Am J Roentgenol. 2000; 175:541–4.
33. Savoca CS. Stress fractures: a classification of the earliest radiographic signs. Radiology. 1971;100: 519–24.
34. Greaney RB, Gerber FH, Laughlin RL, Kmet JP, Metz CD, Kilcheski TS, et al. Distribution and natural history of stress fractures in U.S. Marine recruits. Radiology. 1983;146:339–46.
35. Miller T, Kaeding CC, Flanigan D. The classification systems of stress fractures: a systematic review. Phys Sportsmed. 2011;39:93–100.
36. Kaeding CC, Miller T. The comprehensive description of stress fractures: a new classification system. J Bone Joint Surg Am. 2013;95:1214–20.
37. Geijer M, Borjesson AM, Gothling JH. Clinical utility of tomosynthesis in suspected scaphoid fractures. A pilot study. Skeletal Radiol. 2011;40:863–7.
38. Ottenin MA, Jacquot A, Grospretre O, Noel A, Lecocq S, Louis M, et al. Evaluation of the diagnostic performance of tomosynthesis in fractures of the wrist. AJR Am J Roentgenol. 2012;198:180–6.
39. Fottner A, Baur-Melnyk A, Birkenmaier C, Jansson V, Durr HR. Stress fractures presenting as tumours: a retrospective analysis of 22 cases. Int Orthop. 2009; 33:489–92.
40. Moran DS, Evans RK, Hadad E. Imaging of lower extremity stress fracture injuries. Sports Med. 2008; 38:345–56.
41. Zwas ST, Elkanovitch R, Frank G. Interpretation and classification of bone scintigraphic findings in stress fractures. J Nucl Med. 1987;28:452–7.
42. Roub LW, Gumerman LW, Hanley EN, Clark MW, Goodman M, Herbert DL. Bone stress: a radionuclide imaging perspective. Radiology. 1979;132:431–8.
43. Nussbaum AR, Treves ST, Micheli L. Bone stress lesions in ballet dancers: scintigraphic assessment. AJR Am J Roentgenol. 1998;150:851–5.
44. Matheson GO, Clement DB, McKenzie DC. Scintigraphic uptake of 99mTc at non-painful sites in athletes with stress fractures: the concept of bone strain. Sports Med. 1987;4:65–75.
45. Bryant LR, Song WS, Banks KP, Bui-Mansfield LT, Bradley YC. Comparison of planar scintigraphy alone and with SPECT for the initial evaluation of femoral neck stress fracture. AJR Am J Roentgenol. 2008; 191:1010–5.
46. Campbell R, Grainger A, Hide I, Papastefanou S, Greenough C. Juvenile spondylolysis: a comparative analysis of CT, SPECT, and MRI. Skeletal Radiol. 2005;34:63–73.
47. Bellah R, Summerville D, Treves S, Micheli L. Low-back pain in adolescent athletes: detection of stress injury to the pars interarticularis with SPECT. Musculoskelet Radiol. 1991;180:509–12.
48. Collier B, Johnson R, Carrera G, Meyer G, Schwab J, Flatley T. Painful spondylolysis or spondylolisthesis studied by radiography and single-photon-emission computed tomography. Radiology. 1985;154:207–11.
49. Leone A, Cianfoni A, Cerase A, Magarelli N, Bonomo L. Lumbar spondylolysis: a review. Skeletal Radiol. 2011;40:683–700.
50. Schneiders AG, Sullivan SJ, Hendrick PA, Hones BD, McMaster AR, Sugden BA, et al. The ability of clinical tests to diagnose stress fractures: a systematic review and meta-analysis. J Orthop Sports Phys Ther. 2012;42:760–71.
51. Bianchi S, Luong DH. Stress fractures of the ankle malleoli diagnosed by ultrasound: a report of 6 cases. Skeletal Radiol. 2014;43:813–8.
52. Papalada A, Malliaropoulos N, Tsitas K, Kiritsi O, Padhiar N, Del Buono A, et al. Ultrasound as a primary evaluation tool of bone stress injuries in elite track and field athletes. Am J Sports Med. 2012;40:915–9.
53. Muthukumar T, Butt SH, Cassar-Pullicino VN. Stress fractures and related disorders in foot and ankle: plain films, scintigraphy, CT, and MR imaging. Semin Musculoskelet Radiol. 2005;9:210–26.
54. Vannier MW, Hildebolt CF, Gilula LA, Pilgram TK, Mann F, Monsees BS, et al. Calcaneal and pelvic fractures: diagnostic evaluation by three-dimensional computed tomography scans. J Digit Imaging. 1991; 4:143–52.
55. Lee S, Anderson RB. Stress fractures of the tarsal navicular. Foot Ankle Clin. 2004;9:85–104.
56. Standaert CJ, Herring SA, Halpern B, King O. Spondylolysis. Phys Med Rehabil Clin N Am. 2000; 11:785–803.

57. Kayser F, Resnick D, Haghighi P. Evidence of subperiosteal origin if osteoid osteomas in tubular bones: analysis by CT and MR imaging. AJR Am J Roentgenol. 1998;170:609–14.
58. Gaeta M, Minutoli F, Vinci S, Salamone I, D'Andrea L, Bitto L, et al. High-resolution CT grading of tibial stress reactions in distance runners. AJR Am J Roentgenol. 2006;187:788–93.
59. Feydy A, Drape J, Beret E, et al. Longitudinal stress fractures of the tibia: comparative study of CT and MR imaging. Eur Radiol. 1998;8:598–602.
60. Sievanen H, Koskue V, Rauhio A, Kannus P, Heinonen A, Vuori I. Peripheral quantitative computed tomography in human long bones: evaluation of in vitro and in vivo precision. J Bone Miner Res. 1998;13:871–82.
61. Findlay SC, Eastell R, Ingle BM. Measurement of bone adjacent to tibial shaft fracture. Osteoporos Int. 2002;13:980–9.
62. Wehrli FW, Saha PK, Gomberg BR, Song HK, Snyder PJ, Benito M, et al. Role of magnetic resonance for assessing structure and function of trabecular bone. Top Magn Reson Imaging. 2002;13:335–55.
63. Arendt EA, Griffiths HJ. The use of MR imaging in the assessment and clinical management of stress reactions of bone in high-performance athletes. Clin Sports Med. 1997;16:291–306.
64. Uhmans HR, Kaye JJ. Longitudinal stress fractures of the tibia: diagnosis by magnetic resonance imaging. Skeletal Radiol. 1996;25:319–24.
65. Lee JK, Yao L. Stress fractures: MR imaging. Radiology. 1988;169:217–20.
66. Wieners G, Detert J, Steritparth F, Pech M, Fischbach F, Burmester G, et al. High-resolution MRI of the wrist and finger joints in patients with rheumatoid arthritis: comparison of 1.5 Tesla and 3.0 Tesla. Eur Radiol. 2007;17:2176–82.
67. Niva MH, Sormaala MJ, Kiuru MJ, Haataja R, Ahovuo JA, Pihlajamaki HK. Bone stress injuries of the ankle and foot: an 86-month magnetic resonance imaging-based study of physically active young adults. Am J Sports Med. 2007;35:643–9.
68. Sormaala MJ, Niva MH, Kiuru MJ, Mattila VM, Pihlajamaki HK. Stress injuries of the calcaneus detected with magnetic resonance imaging in military recruits. J Bone Joint Surg Am. 2006;88:2237–42.
69. Kiuru MJ, Pihlajamaki HK, Perkio JP, Ahovuo JA. Dynamic contrast-enhanced MR imaging in symptomatic bone stress of the pelvis and lower extremity. Acta Radiol. 2001;42:277–85.
70. Nachtrab O, Cassar-Pullicino VN, Lalam R, Tins B, Tyrrell PN, Singh J. Role of MRI in hip fractures, including stress fractures, occult fractures, avulsion fractures. Eur J Radiol. 2012;81:3813–23.
71. Behrens SB, Deren ME, Matson A, Fadale PD, Monchik KO. Stress fractures of the pelvis and legs in athletes: a review. Sports Health. 2013;5: 165–74.
72. Swischuk LE, Jadhay SP. Tibial stress phenomena and fractures: imaging evaluation. Emerg Radiol. 2014;21:173–7.
73. Gaeta M, Mileto A, Ascenti G, Bernava G, Murabito A, Minutoli F. Bone stress injuries of the leg in athletes. Radiol Med. 2013;118:1034–44.
74. Navas A, Kassarjian A. Bone marrow changes in stress injuries. Semin Musculoskelet Radiol. 2011;15:183–97.
75. Dixon S, Newton J, Teh J. Stress fractures in the young athlete: a pictorial review. Curr Probl Diagn Radiol. 2011;40:29–44.
76. Cabarrus MC, Amebekar A, Lu Y, Link TM. MRI and CT of insufficiency fractures of the pelvis and proximal femur. AJR Am J Roentgenol. 2008;191: 995–1001.
77. Grangier C, Garcia J, Howarth NR, May M, Rossier P. Role of MRI in the diagnosis of insufficiency fractures of the sacrum and acetabular roof. Skeletal Radiol. 1997;26:517–24.
78. Shin AY, Morin WD, Gorman JD, Jones SB, Lapinsky AS. The superiority of magnetic resonance imaging in differentiating the cause of hip pain in endurance athletes. Am J Sports Med. 1996;24:168–76.
79. Fredericson M, Bergman G, Hoffman KL, Dillingham MS. Tibial stress reaction in runners: correlation of clinical symptoms and scintigraphy with a new magnetic resonance imaging grading system. Am J Sports Med. 1995;23:472–81.
80. Kijowski R, Choi J, Shinki K, Munoz Del Rio a, De Smet A. Validation of MRI classification system for tibial stress injuries. AJR Am J Roentgenol. 2012;198:878–84.
81. Disler DG, McCauley TR, Ratner LM, Kesack CD, Cooper JA. In-phase and out-of-phase MR imaging of bone marrow: prediction of neoplasia based on detection of coexistent fat and water. AJR Am J Roentgenol. 1997;169:1438–47.
82. Kornaat PR, de Jonge MC, Maas M. Bone marrow edema-like signal in the athlete. Eur J Radiol. 2008; 67:49–53.
83. Zubler V, Mengiardi B, Pfirmann CW, Duc SR, Schmid MR, Hodler J, et al. Bone marrow changes on STIR MR images of asymptomatic feet and ankles. Eur Radiol. 2007;17:3066–72.
84. Bergman AG, Fredericson M, Ho C, Matheson GO. Asymptomatic tibial stress reactions: MRI detection and clinical follow-up in distance runners. AJR Am J Roentgenol. 2004;183:635–8.